Integration of Multiple Wave Models from Generation-Scale to Nearshore-Scale: A Practical Application in Maine, USA

Kirk F. Bosma and Brian A. Caufield

Woods Hole Group
81 Technology Park Drive
East Falmouth, Massachusetts, USA 02536
508-540-8080

1. INTRODUCTION

The impact of waves in the nearshore environment, specifically on shorelines that are highly populated or serve significant recreational and/or economic benefits, is one of the key reasons for the continued study of wave propagation, transformations, and predictions. The impact of waves on nearshore processes and shoreline change is highly dependent on the offshore wave climate and the transformation of waves propagating to the shoreline. However, in-depth, complex modeling systems starting from a generation-scale basis are seldom applied in a practical design setting. In many cases, a single design wave condition is selected and/or minimal wave modeling is performed to design and construct shoreline protection (coastal structures, beach nourishment, etc.). This paper presents a successful application of advanced wave modeling techniques to solve a practical coastal engineering problem.

The region of Saco and Camp Ellis Beach, Maine, which is located adjacent to federally constructed and maintained navigational structures (Saco River Jetties), represents a complex coastal setting that has not been well understood (Figure 1). The highly irregular offshore bathymetry, nearby islands, tidal shoals, 3 to 4-meter tide range, mile-long coastal structures, and crenulate-shape of Saco Bay all influence wave propagation in the vicinity of Camp Ellis Beach and the Saco River Jetties. Camp Ellis Beach has been eroding for 150 years. Significant studies of the region have been performed [1-3,6,12-14,21-24,28-32,36,39,41-45], including physical models, engineering analysis, and geological assessment, but have provided conflicting viewpoints and left the local community with no resolution to the ongoing erosion. In an effort to mitigate the erosion, the United States Army Corps of Engineers (USACE) decided that a more rigorous numerical modeling approach, evaluating waves from a generation-scale to nearshore-scale, was required to potentially provide a definitive resolution to the decade long analysis. In this particular case, high-level numerical modeling and science functioned not only to understand the physical processes at work, but also produced a design solution to an erosion problem plaguing a community. The use of sound science and advanced modeling also helped unify previously conflicted stakeholders.

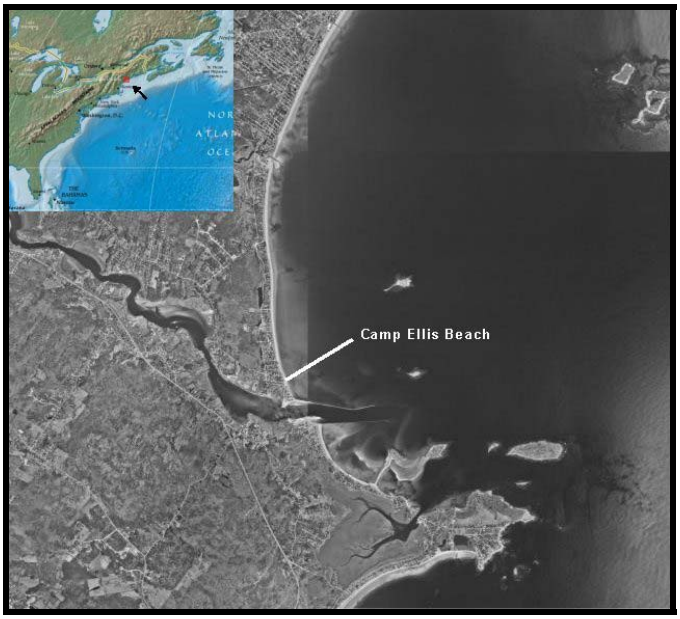

Figure 1. Saco Bay, Saco River and Camp Ellis Beach, Maine, USA.

This paper focuses on the discussion of the overall wave modeling program, and specifically the integration of multiple wave models at various spatial scales. Therefore, detailed discussions of model results within this paper are limited. Each individual model, as well as additional project components (e.g., nearshore circulation modeling, sediment transport modeling, alternatives analysis, field data collection program, input conditions development, etc.), likely deserves stand alone, detailed, in-depth discussion. However, the goal of the current paper is to discuss the success of the model linkage and the plausibility of using a complex modeling system for practical engineering design.

2. BACKGROUND

The Saco River estuary is located at the southern end of a sandy barrier system within the Saco Embayment, in southern Maine, USA (Figure 1). The river is one of the largest rivers in southern Maine and gives rise to the state's largest beach and salt marsh system [22,23]. Due to the rocky nature of the majority of the New England coastline, tidal inlet and barrier development in the region is related to isolated glacial and riverine sediment supplies. Barriers and tidal inlets in

southern Maine, like Saco Bay, are associated with major river systems due to the abundance of sand transported to the coast by these rivers since deglaciation [14]. Historically, navigation within the inlet had been difficult due to the presence of a significant tidal delta at the inlet mouth. Deposition at the inlet created shallow sandbars and ledges that required significant navigation in order to traverse the harbor. The problem became more acute during the mid-19th century as the Biddeford and Saco mills began to import coal and export textile goods [24].

In response to increasing traffic in the area the United States Army Corps of Engineers (USACE) began altering the inlet in 1827 and continued to construct/modify structures in the region until 1969. Currently the inlet is stabilized by a 2030 meter jetty on the northern side, and 1463 meter jetty to the south of the entrance. Maine Geological Survey has classified Camp Ellis Beach as highly erosional [29]. To date, erosion at Camp Ellis Beach has been responsible for the loss of more than 30 homes and repetitive storm damage to roads and streets [39]. The northern structure is highly reflective, with well-placed, interlocking armor units, smooth faces, and steep side slopes.

Over the last half century, the erosion at Camp Ellis Beach has been both a significant concern and heavily debated. Uncertainty over the dominant direction of sediment transport, wave transformations and processes (e.g., mach-stem effects, wave reflection), potential sources of sediment, and the fate of the eroded material, created a division between local scientists, engineers, politicians, and citizens. Under the Section 111 Authority, the USACE undertook a detailed evaluation of the erosion at Camp Ellis Beach. Woods Hole Group was contracted to perform an extensive field data collection and numerical wave modeling program to evaluate the wave transformations, local sediment transport pathways, and identify and assess impacts of potential alternatives to mitigate the erosion at Camp Ellis Beach.

3. FIELD DATA COLLECTION

A wide variety of field measurements were collected during March to June of 2003, including bathymetry, tides, nearshore currents, and waves.

3.1 Bathymetry Measurements

A significant amount of bathymetric information was required to simulate the sea state from the large, coarser grids of the generation scale model to the smaller, finer grids of the nearshore models. Existing data sources were used extensively and supplemented with new surveys for the nearshore region. The generation scale modeling used 30 arc-second bathymetry constructed by the Coastal and Marine Geology Program of the United States Geological Survey. The digital bathymetry was constructed using various data sources:

- NOAA Hydrographic Survey Data and NGDC Marine Trackline Geophysics Data
- Naval Oceanographic Office Digital Bathymetric Data Base - Variable Resolution gridded bathymetry
- Supplemental Datasets from Bedford Institute of Oceanography and Brookhaven National Laboratory
- NOAA Medium resolution digital Shoreline and DMA World Vector Shoreline
- Defense Mapping Agency ETOPO5 Digital relief of the Surface of the Earth
- GEBCO General Bathymetric Chart of the Oceans
- USGS North American 30 arc-second Digital Elevation Model (DEM)

The transformation scale modeling used digital bathymetry from the National Ocean Service (NOS), combined with 1-m LIDAR data [16], as shown in Figure 2, and a high-resolution nearshore bathymetric survey conducted near the mouth of the Saco River on May 13 and 15, 2003 (Figure 3). The LIDAR and new nearshore bathymetric data were also used in the local and nearshore wave simulations.

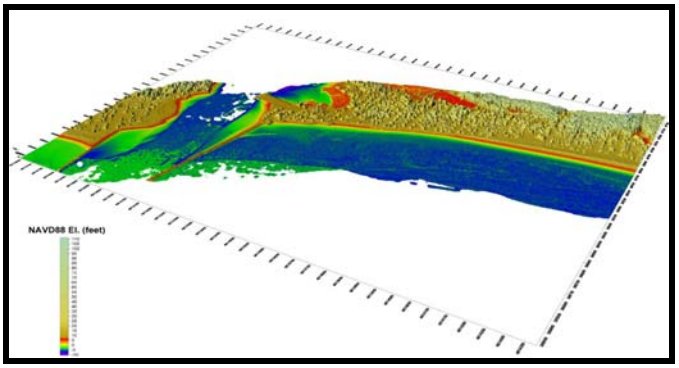

Figure 2. 1-meter LIDAR data of Camp Ellis region.

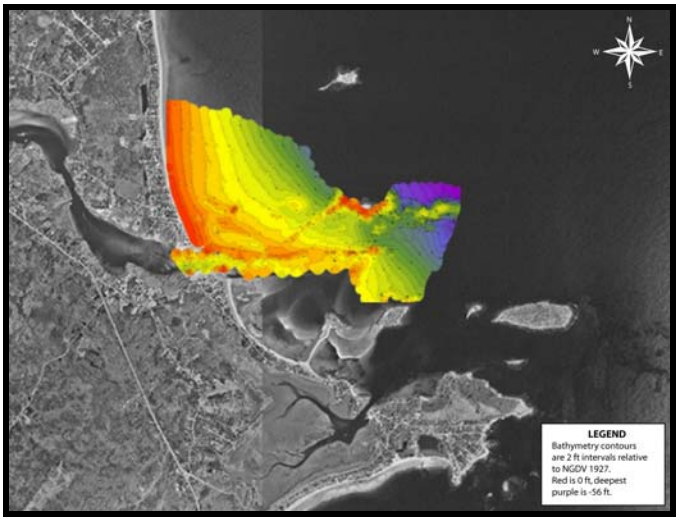

Figure 3. Nearshore bathymetric data collected in May, 2003.

3.2 Wave Measurements

In order to calibrate, verify, and validate the numerical wave modeling system, wave data were measured at two locations within the nearshore zone. The collection program incorporated using two bottom-mounted Acoustic Doppler Current Profilers (ADCP). The ADCPs recorded directional wave information every hour from 12 March to 21 May 2003. The ADCPs also collected directional current information and water levels every 10 minutes. A Workhorse Sentinel 600 kHz ADCP was placed in the region seaward of Eagle and Ram Islands (43º28.60' N, 070º 20.48' W) in approximately 17 m of water (Figure 4). A second system, a Workhorse Sentinel 1200 kHz ADCP, was placed in a region landward of Eagle and Ram Island (43º28.31' N, 070º22.42' W) in approximately 4 m of water (Figure 4). The system locations were selected to determine the potential impacts of the nearshore islands on the local wave transformations.

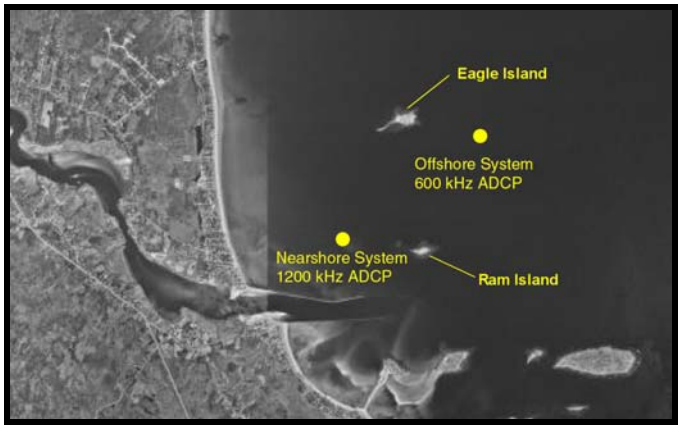

Figure 4. Location of wave observation systems within Saco Bay.

The Workhorse Sentinel ADCP uses a four-beam array, 20º from vertical, in a convex configuration. A complete frequency-direction wave spectrum is measured and is capable of resolving multiple wave directions arriving with the same frequency. The ADCPs record accurate wave statistics by correcting for bias effects due to wave/current interaction and directional averaging (accuracies within 0.25 to 1% of full scale). Since the systems operate on the sea floor, there was a significantly lower risk of loss or damage in the nearshore environment that is heavily used by boaters and fisherman. The nearshore system was capable of resolving waves with a 1.8 second period, while the offshore system was able to resolve waves with a 2.9 second period. The ADCPs measured waves in 20 minute long bursts every hour. Data recovery was 100% for both systems.

Figure 5 presents the significant wave height results for the two ADCP stations, as well as the non-direction NOAA buoy (44007) offshore of Portland, Maine. The results indicated the wave height decay with the propagation shoreward.

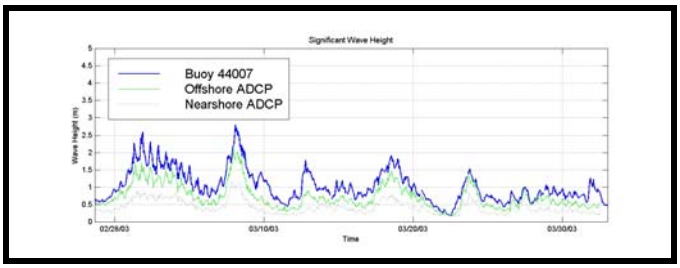

Figure 5. Comparisons of significant wave height results for the offshore and nearshore ADCPs and the Portland NOAA buoy (44007).

Figure 6 presents the percentage frequency of occurrence of peak wave period (seconds) and peak wave direction (degrees from north) observed at the offshore station. The contour lines indicate the location of higher percentages. Total percentages of directional and period bins are shown at the far right and bottom of each figure. The figure indicates that a majority of the wave periods are between 7 and 10 seconds (54.3%). A total of 41.9% of the waves are between 7 and 10 seconds and approach from between 79 and 124 degrees. A high percentage (23.6%) of the 8-10 second waves are arriving from between 101 and 124 degrees. A secondary peak (7.1%) of waves between 6 and 7 seconds are coming from between 124 and 146 degrees. The directional spreading of the wave period is limited during this deployment, as indicated by the tightly focused contour lines.

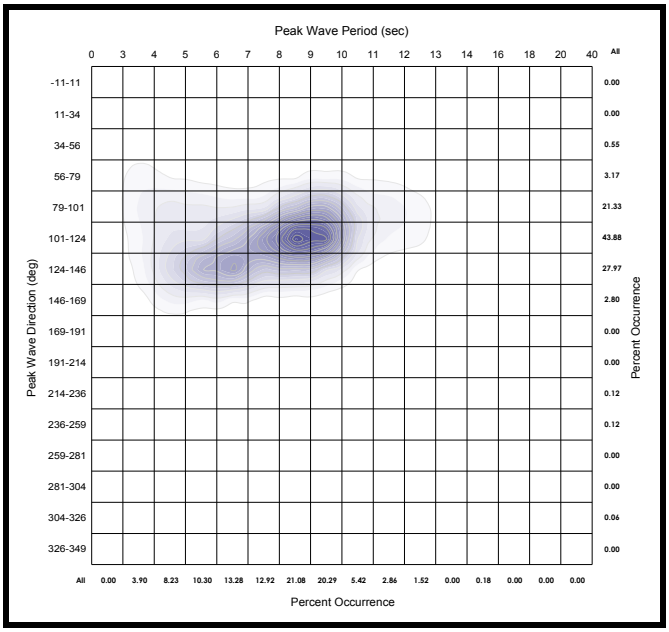

Figure 6. Percentage frequency of occurrence statistics of peak period versus peak wave direction for the offshore station.

Figure 7 presents a similar plot for the nearshore wave station. In addition to the As the wave propagate between the islands, the waves transform into a nearly unidirectional approach to the shoreline, as waves consistently arrive from between 79-101 degrees independent of their offshore direction.

Existing wave observations were also utilized to assist in calibration, verification, and validation, as well as provide longer temporal coverage. These sources included Wave Information Systems (WIS) wind-wave hindcast data, NOAA buoys (non-directional), and Gulf of Maine Ocean Observing System (GoMOOS) buoys (non-directional).

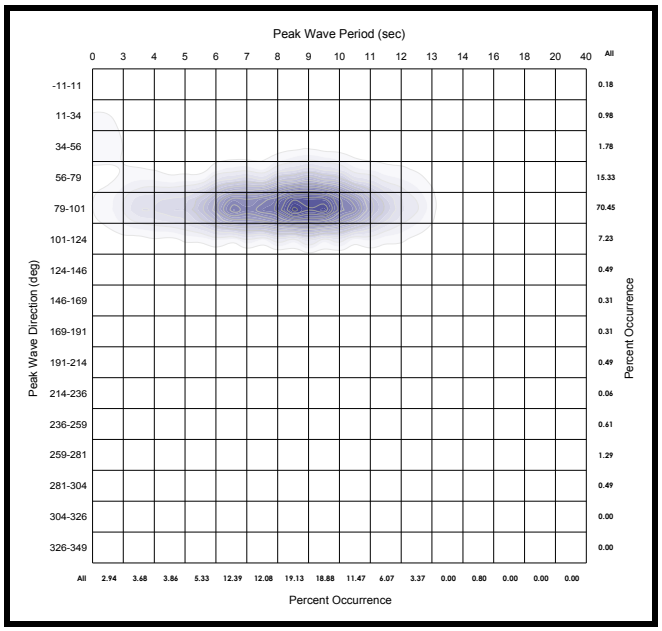

Figure 7. Percentage frequency of occurrence statistics of peak period versus peak wave direction for the nearshore station.

3.3 Supplementary Measurements

Tidal elevations were measured at 4 (four) locations throughout the river and bay system, while nearshore currents were observed via both the wave ADCP systems and a boat-based survey to evaluate spatial variations. These observations are not discussed as part of the current paper, but were utilized in the overall project program.

For example, complicating the region is over a 3-meter tidal range, requiring model simulations to be conducted relative to both low and high tide levels.

4. WAVE MODELING SYSTEM

A comprehensive numerical wave modeling system was developed for the Saco Bay area. The modeling system is able to simulate wave conditions from generation-scale (utilizing satellite wind data), through transformation-scale, to local scale, to high resolution Boussinesq modeling. Each subsequent model builds on the results from the previous model. Spectral input conditions were passed forward at each transition, with each model progression resulting in an increase in resolution, added complexity, and incorporation of additional wave dynamics and structural interactions. Each model was calibrated, verified, and/or validated. Validated models were then used to evaluate potential alternatives for reducing wave energy, and subsequently sediment transport, in the Camp Ellis region. The entire modeling system; therefore, consists of the integration of multiple validated wave models taking waves from offshore generation to the interaction at the coastline.

3.1 Generation Scale Modeling

In many cases, wave input conditions for nearshore wave transformation modeling can be obtained directly from offshore wave buoys. However, in order to calibrate, verify, and validate the wave modeling system within Saco Bay, offshore directional wave information was required concurrently with the nearshore wave observations (March-May 2003). Although there are significant wave observations within the Gulf of Maine, the data are all non-directional. Therefore, buoy data have limited use as a boundary condition for calibration of the transformation models. Existing Wave Information System (WIS) wind-wave hindcast data contained directional spectra, but the current database only extends to 1999. To improve upon these limitations, satellite wind fields and an offshore, spectral, wave generation model was applied for the time period of the field data collection program (March-May 2003) to provide spectral wave input conditions directly at the boundary of the regional wave model.

The spectral wave model, WAVAD [35], was used for the generation scale modeling. WAVAD is based on a f-4 equilibrium range formulation, as supported by field experiments [15,20,25,40] and is consistent with energy conservation in the equilibrium range, as calculated from the complete or reduced Boltzmann integrals. In a coordinate system moving with the group velocity of the spectral peak, the governing equation for the evolution of the wave spectrum can be approximated as:

$$\frac{DE(f)}{Dt} = \sum_{i=1}^{6} S_n(f) \qquad \textbf{(1)}$$

Where Sn(f) represents a separate source term:

$S_1(f)$ = shoaling,
$S_2(f)$ = refraction,
$S_3(f)$ = wind effects,
$S_4(f)$ = wave-wave interactions
$S_5(f)$ = bottom interaction effects

The WAVAD model represents each of these processes using state-of-the-art methodologies developed from theory and experiments. The fetch-growth characteristics of the model are similar to the JONSWAP relationships (i.e., wave energy increased linearly with fetch) and the duration-growth characteristics are roughly similar to those of Resio [33] and the Navy's Spectral Ocean Wave Model (SOWM).

The model used input wind fields as the primary generating force for deep-water waves. The wind fields were created

using the data from the National Aeronautics and Space Administration's QuikSCAT satellite. This satellite houses a microwave scatterometer (SeaWinds) designed specifically to measure near-surface wind velocity (both speed and direction) over the global oceans under all weather conditions [18]. A series of two nested grids was applied to simulate the time period spanning the deployment of the two ADCPs. The larger grid has a resolution of 0.25 decimal degrees (17.9 miles), while the nested grid has 0.05 decimal degrees (3.5 miles).

WAVAD output included wave spectra at equi-spaced points within the area of interest. The modeled wave spectra represented the distribution of wave energy with respect to frequency, and were represented as fully three-dimensional spectra in discretized frequency and direction bands. Propagation effects and source/sink mechanisms were computed in terms of variations in energy levels in each of these frequency-direction elements. All wave parameters such as significant wave height, frequency of the spectral peak, and mean wave direction were computed from these discrete elements. Spectral wave output from the WAVAD model was used as input into the transformation-scale wave model (STWAVE) for calibration and verification time periods. Details on the generation scale modeling can be found in Caufield and Bosma [9].

3.2 Transformation-Scale Wave Modeling

The spectral wave model STWAVE version 3.0 [37] was used to transform the data from the generation scale results into the nearshore environment and to provide input into the local wave model. STWAVE is a steady-state, spectral wave transformation model, based on a form of the wave action balance equation of Jonsson [19].

$$(C_{ga})_i \frac{\partial}{\partial x_i} \frac{C_a C_{ga} \cos(\mu - \alpha) E(\omega_a, \alpha)}{\omega_r} = \sum \frac{S}{\omega_r} \qquad (2)$$

where

i = x,y spatial coordinates
C_a = absolute wave celerity
C_{ga} = absolute wave group celerity
μ = current direction
α = propagation direction of spectral component
E = spectral energy density
f = frequency of spectral component
T_r = relative angular frequency (frequency relative to current)
S = energy source/sink terms

Source and sink terms include wind input, nonlinear wave-wave interactions, dissipation in the wind field, and surf-zone breaking. The model can simulate wave refraction and shoaling induced by changes in bathymetry and by wave interactions with currents. The model also includes wave breaking, wave growth, and influences of wave white capping on the distribution and dissipation of energy in the wave spectrum. Model outputs include zero-moment wave height, peak wave period, and mean wave direction at all grid points and two-dimensional spectra at selected grid points. A comprehensive discussion of the theoretical background of STWAVE, including limitations and assumptions, can be found in Smith, Sherlock, and Resio [37].

The STWAVE model domain consists of one reference grid covering the entire region of Saco Bay. The bathymetric grid is rotated to create an x-axis perpendicular to the shoreline (waves from 120 degrees are parallel to the x-axis) and extends from the shoreline to an offshore node of the WAVAD generation-scale model and WIS Station 99 and (for annual average simulations). This offshore boundary corresponded to an approximate depth of 35 to 40 meters. The STWAVE grid consists of 290 cells across the shore and 347 cells along the shore with a resolution of 30.5 meters (100 feet). Figure 8 shows the location and geometry of the reference grid.

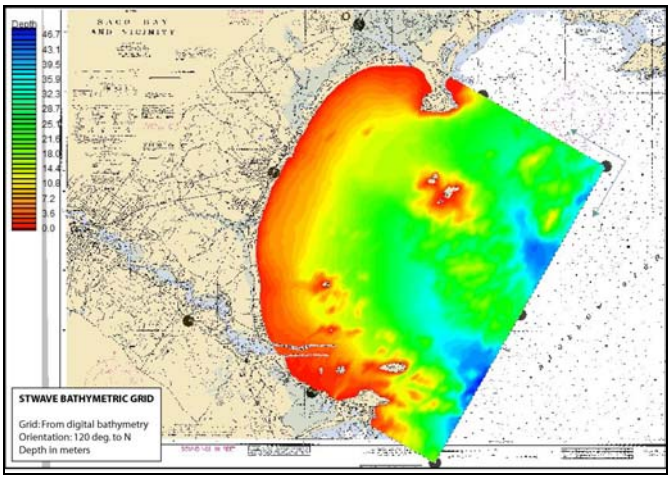

Figure 8. Bathymetric grid used for the STWAVE modeling.

Transformation wave modeling results can only be as accurate as the input data; therefore, a key component of accurate wave modeling is the analysis and selection of input wave data. STWAVE simulates the behavior of a random sea surface by describing wave energy density as a function of direction (directional spectrum) and frequency (frequency spectrum). The two-dimensional wave spectrum is discretized into separate wave components, which constitute an essential part of the input for STWAVE. The two-dimensional wave spectrum is given as the product of the energy and directional spectra. Through a combination of the various wave directions and frequencies, STWAVE is able to simulate the behavior of a natural, random sea. In addition, detailed analysis and selection of input spectrum allows the model to assess the impact of different seasonal conditions, varying wave approach pathways, and storms. Spectral results from calibration and verification of WAVAD were used directly as input into STWAVE for model validation.

Bulk wave parameters (parametric methods) were not utilized to generate input conditions in either validation or in average annual wave condition simulations. Spectral conditions derived from parametric methods (e.g., TMA spectra, $\cos^n$ directional distribution) result in larger errors in calculation of peak period and wave direction (Smith and Gravens 2003).

In order to determine long-term wave conditions and for use in sediment transport calculations, spectral data from WIS Station 99 (Phase II) and 38 (Phase III) were used to derive energy-conserving annual average directional spectrum. Data are segregated by direction of approach, and an energy distribution, as a function of frequency, is generated from all the waves in each directional bin. The energy associated with each frequency is then summed to create an energy distribution for each approach direction. In essence, a representative two-dimensional spectrum is generated for each approach directional bin based on the sum of all the WIS spectra approaching from that mean direction. This is combined with the percentage of occurrence to create a long-term (10-20 year) evaluation of wave impacts at the shoreline. This energetic directional bin approach has been successfully utilized in transformation modeling [8,17] and identifies all potential approach direction, including those that may occur only a small percentage of time during a typical year, but potentially have significant impacts on the shoreline.

In addition, STWAVE is a half-plane model, and therefore, only represents waves propagating towards the coast. Waves that may be reflected from the coastline or structures and waves that are generated by winds blowing offshore are not included. STWAVE, therefore, only represents an intermediate step in the wave modeling system and is not used for local sediment transport calculations for the Camp Ellis region. Due to STWAVE limitations, it was important to advance to higher-resolution models that embodied the reflection processes and could more accurately determine the nearshore structural interactions.

3.3 Nearshore Wave Modeling

The STWAVE model results identified the regional Saco Bay wave transformations; however, due to the complex bathymetry in the vicinity of the Camp Ellis Beach, the nearshore islands, the jetties themselves, and the need to evaluate a number of complex alternatives, a higher resolution model, encompassing additional wave processes, was required. Two-dimensional spectral output from STWAVE was used as input into the local, nearshore wave model. The nearshore wave model, CGWAVE, is utilized to evaluate the local physical processes (e.g., wave reflection, wave-induced currents, wave dispersion, nearshore wave refraction and diffraction, etc.), and subsequently the engineering alternatives.

The physics embodied in CGWAVE [10] are based on solving the two-dimensional elliptic mild-slope equation [4,5].

$$\nabla \bullet \left(CC_g \nabla \hat{\eta}\right) + \frac{C_g}{C}\sigma^2 \hat{\eta} = 0 \qquad \textbf{(3)}$$

where

η=complex surface elevation function, from which the wave height can be determined

σ=wave frequency under consideration (radians/second)

C=phase velovity= σ/k

C_g=group velocity =$\partial\sigma/\partial k$=nC

$$n = \frac{1}{2}\left(1 + \frac{2kd}{\sinh\left(2kd\right)}\right) \qquad \textbf{(4)}$$

k=wave number ($2\pi/L$), related to the local depth (d) through the linear dispersion relation:

Equation 1 simulates wave refraction, diffraction and reflection in coastal domains of arbitrary shape. The mild slope equation can be modified to account for the effects of frictional dissipation and wave breaking:

$$\nabla \bullet \left(CC_g \nabla \hat{\eta}\right) + \left(\frac{C_g}{C}\sigma^2 + i\sigma w + iC_g \sigma\gamma\right)\hat{\eta} = 0 \qquad \textbf{(5)}$$

where w is a friction factor and γ is the wave breaking parameter.

It is also possible to account for non-linear wave mechanics in CGWAVE. The mild-slope equation is modified by using a non-linear dispersion relation instead of the linear relation.

$$\sigma^2 = gk\left\{1 + \left(ka\right)^2 F_1 \tanh^5\left(kd\right)\tanh\left(kd + kaF_2\right)\right\} \qquad \textbf{(6)}$$

where:

$$F_1 = \frac{\cosh\left(4kd\right) - 2\tanh^2\left(kd\right)}{8\sinh^4\left(kd\right)} \qquad \textbf{(7)}$$

$$F_2 = \left(\frac{kd}{\sinh\left(kd\right)}\right)^4 \qquad \textbf{(8)}$$

To account for the model domain boundaries that are not open water, the model assumes a reflective boundary condition that can be varied for each section of the domain boundary (e.g., coastline, islands, structures, etc.). Along open boundaries where outgoing waves must propagate to infinity, the Sommerfeld radiation condition is applied.

CGWAVE is solved using a finite-element method. The finite-element method is used to model coastal phenomena in a region of complex shape. Figure 9 presents the modeling grid used for the nearshore wave modeling (relative to Mean High Water) consisting of 262,940 nodes and 523,555 elements with approximate dimensions of 3 nautical miles by 3 nautical miles. In the nearshore zone, resolution is approximately 10 meters or 8 nodes per wavelength.

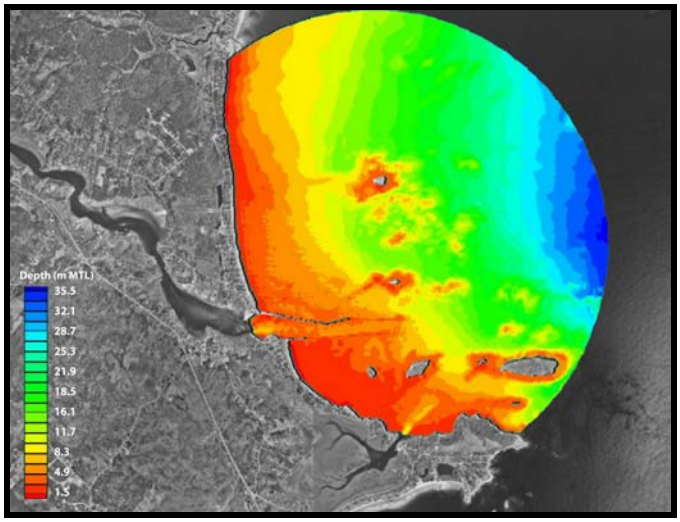

Figure 9. Bathymetric grid used for the CGWAVE modeling.

The nearshore model was simulated using the same set of conditions developed for the transformation scale modeling. Spectral boundary conditions are specified along the offshore radiating boundary using spectral results from STWAVE for calibration and verification time periods, as well as all annual average, directional approach simulations.

3.4 Boussinesq Wave Modeling

Due to the complex nearshore bathymetry, complicated structural configuration(s), and potential for Mach-Stem effects, and in order to simulate final engineering alternatives in more detail, the nearshore environment was simulated using a Boussinesq wave model. Boussinesq wave modeling represents the state-of-science in wave modeling, and is capable of providing the most accurate simulation of the nearshore region. The Boussinesq wave model, MIKE 21-BW [11], is capable of reproducing the combined effects of most wave phenomena of interest in coastal and harbor engineering, including shoaling, refraction, diffraction, and reflection of irregular short-crested and long-crested finite amplitude waves propagating over complex bathymetries. In addition, phenomena such as wave grouping, generation of bound sub-harmonics and near resonant triad interactions, are also simulated. The Boussinesq level modeling was geared at identifying all the physical processes in the immediate study region, with particular focus on the wave-structure interactions. MIKE 21-BW solves the Boussinesq equations using a flux-formulation with improved linear dispersion characteristics. These enhanced Boussinesq type equations [26,27] make simulation of directional wave trains from deep to shallow water feasible.

The bathymetric grid for the Boussinesq model is shown in Figure 10. The grid extends from the shoreline to an offshore boundary corresponding to the offshore ADCP station. The grid consists of 800 cells across the shore and 600 cells along the shore with a resolution of 5 meters. Sponge layers are utilized around the structures, islands, and coastlines to represent varying reflection/transmission influences.

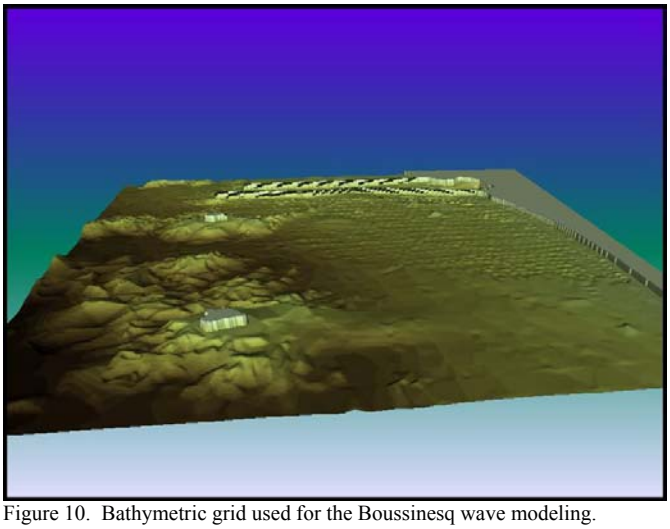
Figure 10. Bathymetric grid used for the Boussinesq wave modeling.

The model was calibrated and verified using spectral data collected at the offshore ADCP station as a boundary condition, and concurrent data at the nearshore ADCP for model/data comparisons. Once calibrated, the Boussinesq model was used to simulate the average annual directional conditions for the same set of conditions developed for the nearshore wave modeling. In these cases, CGWAVE spectral results were passed to the Boussinesq model at the offshore boundary.

5. Model Calibration And Verification

The model system was calibrated, verified, and/or validated for specific time periods in April 2003, during the ADCP deployment. The generation-scale model (WAVAD) was calibrated from April 24-28, 2003 and verified from April 1-7, 2003. Details on the calibration and verification of the generation scale model can be found in Caufield and Bosma [9].

For each time period (calibration and verification), two-dimensional spectral output from WAVAD was used directly as input into STWAVE for validation purposes. Table 1 presents error statistics (bias and RMS error) for the STWAVE simulations based on the offshore and nearshore ADCP stations. The bias and root-mean-square (RMS) error are defined as:

$$Bias = \frac{\sum \left(P_{measured} - P_{simulated} \right)}{n} \quad (9)$$

$$RMS\ Error = \sqrt{\frac{\sum \left(P_{measured} - P_{simulated} \right)^2}{n}} \quad (10)$$

where $P_{measured}$ is the measured wave parameter (ADCP station), $P_{simulated}$ is the modeled wave parameter, and n is the number of values. A positive bias indicates underestimates by the model, while a negative bias indicates an overestimate.

TABLE 1
STWAVE MODEL ERRORS BASED ON ADCP STATIONS.

Wave Parameter	Offshore ADCP Station		Nearshore ADCP Station	
	Bias	RMS Error	Bias	RMS Error
H_S (m)	-0.02 m	0.11 m	-0.21 m	0.22 m
T_p (sec)	0.1 sec	0.2 sec	0.4 sec	0.5 sec
Dir (deg)	11.5 deg	12 deg	9 deg	9.4 deg

Validation results for STWAVE indicated the model results compare to the observed parameters well. Slight over prediction of the wave height at the nearshore ADCP location indicates the potential inability of the model to fully predict the energy losses occurring between the complex bathymetry of the islands. This may be due to the lack of diffraction processes in STWAVE, which are likely important in the lee of the islands. As a secondary validation, two-dimensional observed spectra from the ADCP stations and two-dimensional spectra output from the STWAVE model were compared. Figure 11 shows the visual results of the spectral comparison. Results of the spectra also showed favorable comparison.

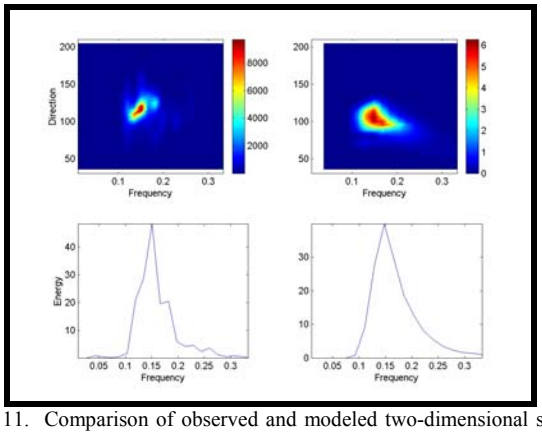

Figure 11. Comparison of observed and modeled two-dimensional spectra. Offshore ADCP station spectra are presented in the left panels, while STWAVE output of modeled spectra are presented in the right panels.

Spectral output from the STWAVE validation runs for the calibration and verification time periods were then used to generate input conditions for the local wave model, CGWAVE. Due to the high resolution of the model domain, similar calibration techniques to those presented in Briggs et al. [7] were used to calibrate and verify the CGWAVE model.

Table 2 presents error statistics (bias and RMS error; equation 9 and 10, respectively) for the CGWAVE calibration based on the offshore and nearshore ADCP stations.

TABLE 2
CGWAVE MODEL ERRORS BASED ON ADCP STATIONS.

Wave Parameter	Offshore ADCP Station		Nearshore ADCP Station	
	Bias	RMS Error	Bias	RMS Error
H_S (m)	0.15 m	0.19 m	0.24 m	0.31 m
Dir (deg)	6.6 deg	8.4 deg	11.5 deg	33.0 deg

The CGWAVE model also compared favorable to observed results, as long as the number of spectral components simulated remains high. Failure to use non-linear terms or use of a reduced number of spectral components resulted in increased errors. The greater the number of spectral components used in the CGWAVE input, the greater the accuracy of the results. The accuracy is slightly less than those shown for STWAVE results due to the increased complexity of the bathymetry, islands, and structures in the nearshore zone.

Finally, the Boussinesq model was calibrated and verified using spectral data collected at the offshore ADCP station as a boundary condition, and concurrent data at the nearshore ADCP for model/data comparisons.

6. WAVE MODELING RESULTS

Following calibration and verification, the transformation scale (STWAVE), local (CGWAVE), and Boussinesq (MIKE 21-BW) models were used to simulate a wide range of annual average directional conditions, return-period storm events, and specific historical storm events. Considering that all cases of annual conditions were simulated for both high and low water, this represents a significant amount of model simulations. Table 3 presents the directional bin scenarios, including the percent occurrence and the percent of the total energy that is contained in each bin, as derived from the WIS data. Waves propagating offshore were not modeled in the system, and were assimilated into the analysis as calm periods.

TABLE 3
DIRECTIONAL SIMULATION CASES

Directional Approach Bin	Percent Occurrence	Percentage of Total Energy
42.5 (30 to 55)	2.44	2.98
65 (55 to 75)	4.32	8.05
82.5 (75 to 90)	3.93	7.99
100 (90 to 110)	9.19	8.41
120 (110 to 130)	17.90	13.84
140 (130 to 150)	22.99	15.92
157.5 (150 to 165)	15.20	10.92
175 (165 to 185)	7.77	10.17
197.5 (185 to 210)	7.40	11.21
Waves Propagating Offshore	8.86	10.56

Figure 12 presents two examples of the two-dimensional spectra input generated from the Phase II WIS data for representation of annual directional bin conditions.

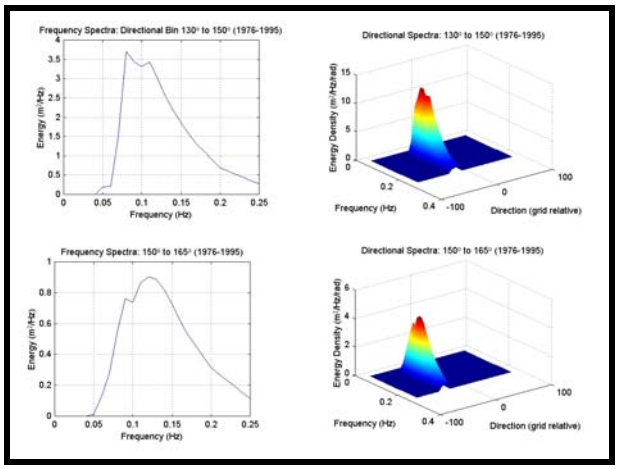

Figure 12. Examples of two-dimensional spectra input into STWAVE for annual average directional simulations. The upper two panels are for waves approaching from between 130 to 150 degrees, while the bottom two panels are for waves approaching from 150 to 165 degrees.

Table 4 presents the storm scenarios simulated. Historical storm parameters were based on historical data observations, while return-period storm parameters were developed using the Generalized Extreme Value (GEV) method. This method provides reliable estimates of extremes without assuming the distribution type is known [34]. Storm spectra were developed from these bulk parameters using standard parametric methods (e.g., TMA spectra, $\cos^n$ directional distribution) since the observed spectra during these events are unknown.

TABLE 4
STORM EVENT SIMULATIONS

Storm Event	Hs (m)	Tp (sec)	Direction (degrees)	Storm Surge (m above MTL)
10-year	6.20	7.9	60	2.4
50-year	7.10	8.5	60	2.6
100-year	7.48	8.7	60	2.7
Perfect Storm (10/31/1991)	6.90	14.3	37	2.4
Hurricane Bob (08/20/1991)	5.80	11.1	-20	1.8
March 6-7, 2001	5.58	11.1	50	2.4

Figure 13 shows an example result from the STWAVE model for the directional bin approach of 110 to 130 degrees (southeast approach). The color map corresponds to the distribution of significant wave height (meters) throughout the model domain. Warm colors (reds and yellows) indicate a higher wave height, while cool colors (blues and greens) indicate a reduced wave height. The STWAVE results were used to generate wave-induced currents (from radiation stresses) and regional sediment transport results for the entire Saco Bay Region (from headland to headland), as well as provide input into the nearshore wave model.

Figure 14 shows example sea surface results from the nearshore wave model (CGWAVE) for a southeastern approach spectrum. Dark blues represent the wave crests, while whites represent the wave troughs. The impact of the nearshore islands, shoals, and structures, as well as diffraction/refraction patterns and the crossing of various wave trains, is clearly evident in the sea surface results.

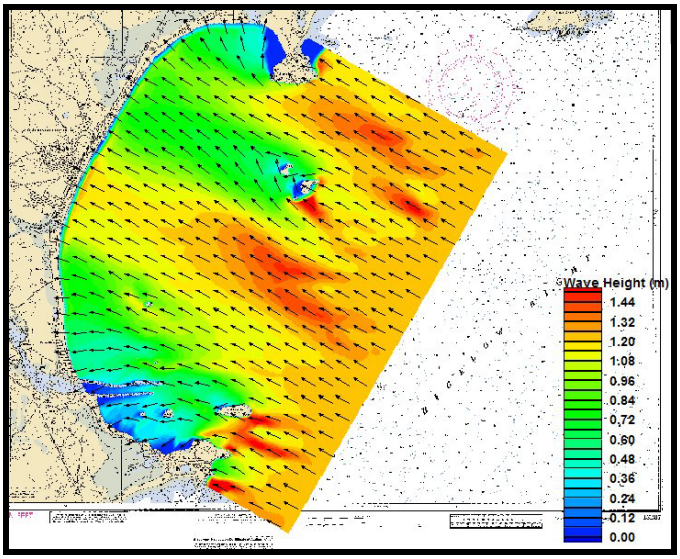

Figure 13. Example of STWAVE modeling results for existing conditions using a southeastern approach directional spectra bin.

Figure 15 presents similar sea surface results in the direct vicinity of Camp Ellis Beach. The color map was modified to represent an entire spectrum of color in order to facilitate visual identification of wave train interaction. The significant wave reflection off of the northern jetty is identified as the waffle type sea surface north of the structure. The Camp Ellis region is impacted by not only the incident wave train propagating between the islands, but also the reflected wave energy from the northern jetty. In nearly all cases, independent of offshore direction of approach, the nearshore waves propagated directly towards the Camp Ellis Beach region and the northern jetty. The transformations occurring due to the complex bathymetry between the islands, and the islands themselves, resulted in a nearly uniform approach towards the region of highest erosion and reflection.

Results from the nearshore wave model (CGWAVE) were utilized to produce local nearshore circulation (from radiation stresses) and sediment transport results, and provide initial screening of the proposed engineering alternatives.

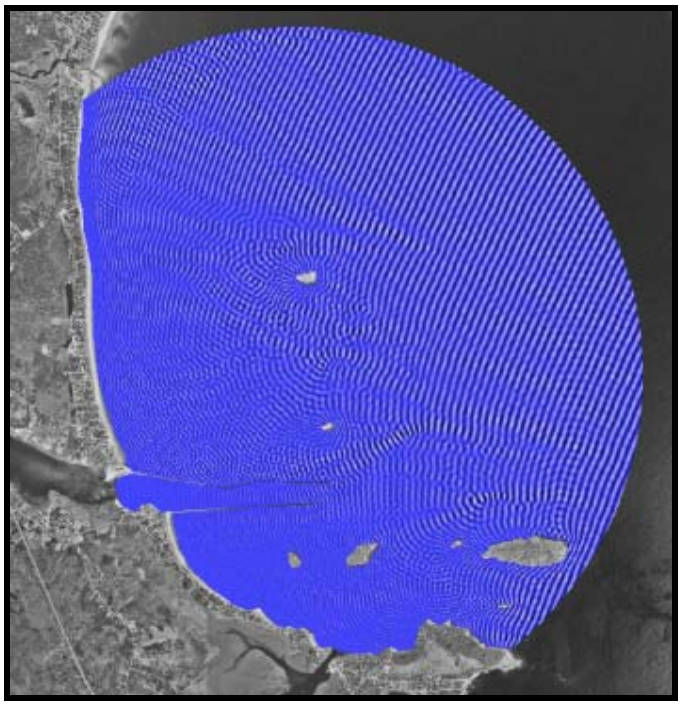

Figure 14. Example results of sea surface output from the nearshore wave model (CGWAVE). The simulation is for a southeastern approach spectrum at Mean Tide Level. Dark blues represent wave crests, while the whites represent wave troughs. Patterns of refraction and diffraction throughout the domain are clearly visible.

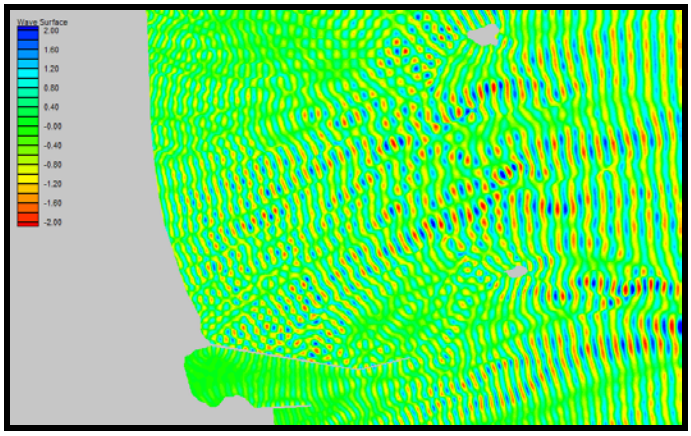

Figure 15. Sea surface results from the CGWAVE model for the 10-year storm conditions in the vicinity of Camp Ellis Beach. Blues indicate wave crests, while reds indicate wave troughs. The reflection off of the northern jetty is clearly visible.

Figure 16 shows an example of sea surface results from the Boussinesq model for a spectral wave approach from the southeast (140 degrees). Again, the wave transformation between the island complex and the reflection from the northern jetty are clearly evident. Results from the Boussinesq model were used in the final screening analysis of the alternatives, as well as to determine beach lifetime performance.

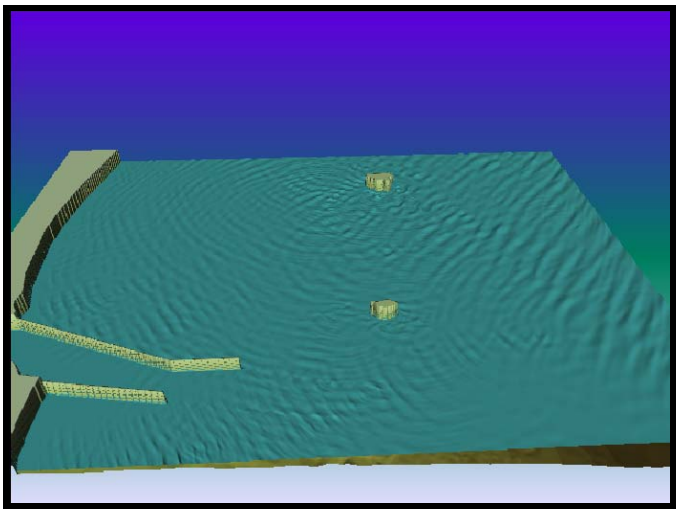

Figure 16. Example sea surface results from the Boussinesq wave model for existing conditions. Wave approach from the southeast (140 degrees).

7. ALTERNATIVE ANALYSIS

The ultimate goal of the modeling system was application towards the evaluation of a wide range of alternatives. The alternatives were geared towards mitigating the ongoing erosion occurring at Camp Ellis Beach. Over twenty (20) potential solutions, including both structural (e.g., spur jetties, breakwaters, groins, etc.) and non-structural (e.g., partial jetty removal, offshore borrow pits, jetty roughening, etc.), were determined jointly between Woods Hole Group, the USACE, and Maine Geological Survey. Table 5 lists the base 20 proposed alternatives. Numerous sub-alternatives were completed in order to optimize placement and basic engineering parameters, as well as simulate salient growth behind coastal engineering structures (by digital modification of the bathymetry).

TABLE 5
BASE PROPOSED ALTERNATIVES

Alternative I.D.	Average Target Strength (targets/m^3)
1	Northern Jetty Extension Removal
2	Northern Jetty Extension Removal and Jetty Lowering
3	750’ Spur Jetty
4	500’ Spur Jetty
5	Dual 500’ Spur Jetties
6	Additional configuration of best performing spur alternative
7	Optimized Spur Jetty Alternative with Northern Jetty Extension Removal
8	Optimized Spur Jetty Alternative with terminal groin
9	T-Head Groins
10	Secondary T-Head Layout
11	Offshore Breakwater
12	Secondary Offshore Breakwater Location
13	Combination of Spurs and Breakwater
14	Multiple Short Spur Jetties
15	Offshore Borrow Pit
16	Borrow Pit and optimized Spur Jetties
17	Jetty Roughening
18	Submerged Breakwater/Shoal
19	Optimized Combination of Spurs and Breakwater
20	750’ Spur Groin, Jetty Roughening, and Extension Removal

Due to the number of simulations required to evaluate all potential solutions, the alternatives analysis consisted of an initial and final screening process. The nearshore wave model (CGWAVE) was used as the initial screening tool through evaluation of changes in wave energy, wave height, and wave direction. Wave energy reduction was evaluated in specific zones in the vicinity of Camp Ellis and the structures (Figure 17). The result in Figure 17 show wave heights (m) for a breakwater alternative as a color map behind the energy evaluation zones.

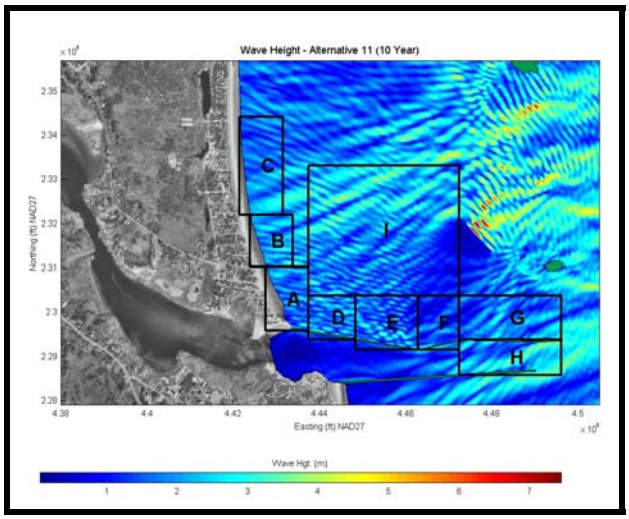

Figure 17. Areas used to evaluate changes in wave energy in the vicinity of Camp Ellis Beach and the Saco River Jetties.

Figures 18 and 19 show examples of the reduction in wave height in CGWAVE for the offshore breakwater alternative and 230-meter (750 foot) spur jetty alternatives, respectively. Differences in wave heights (between existing condition cases and alternative cases) were computed at each node within the CGWAVE model domain. Positive values of wave height change (m) indicate and increase in wave energy, while negative values in wave height change (m) indicate a decrease in wave energy. The four alternatives demonstrating the greatest potential for successfully reducing energy (and thus sediment transport), without resulting in negative impacts, were passed forward to the final screening analysis utilizing the Boussinesq wave model.

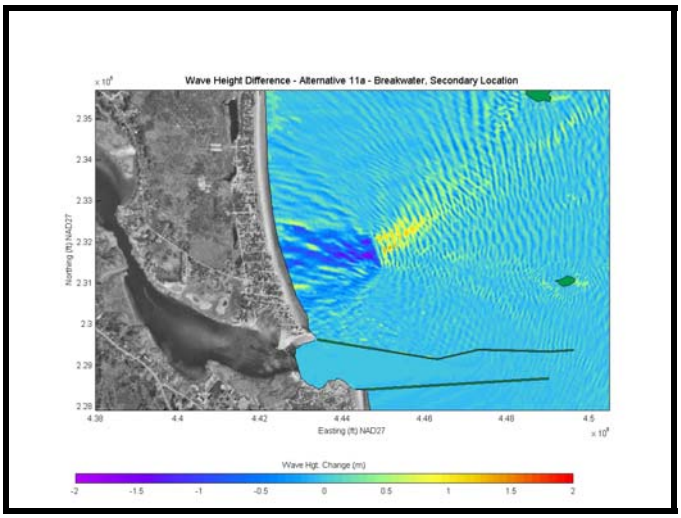

Figure 18. Wave height changes in CGWAVE for a breakwater alternative.

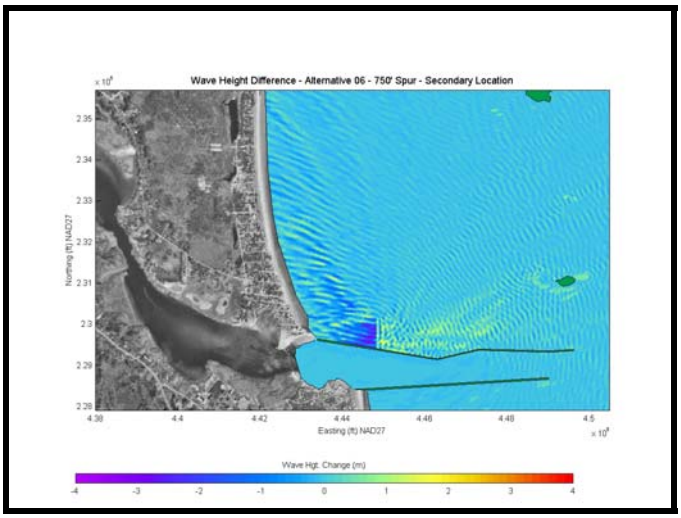

Figure 19. Wave height changes in CGWAVE for a 230-meter spur jetty alternative.

The final screening analysis included simulation of the alternative in the Boussinesq wave model, development of wave-induced nearshore circulation from radiation stresses, and sediment transport evaluation. Figure 20 presents an example (the combined breakwater spur alternative) of the Boussinesq alternative simulations for this final screening. These final alternatives were also evaluated from an economic standpoint on a cost-benefit basis.

The ultimate goal of the overall project was to create a sustainable beach at Camp Ellis Beach through sediment supplied via the maintenance dredging occurring in the Saco River. Approximately 80,000 cubic yards of sediment is removed from the Saco River approximately every 10-years. This material can be used as a direct source to replenish the beach. The proposed alternatives must be able to reduce the erosion to the point that this influx of material is able to maintain a beach capable of providing wave and flooding protection. The wave modeling system results were the key

input into the sediment transport modeling and beach nourishment performance evaluation.

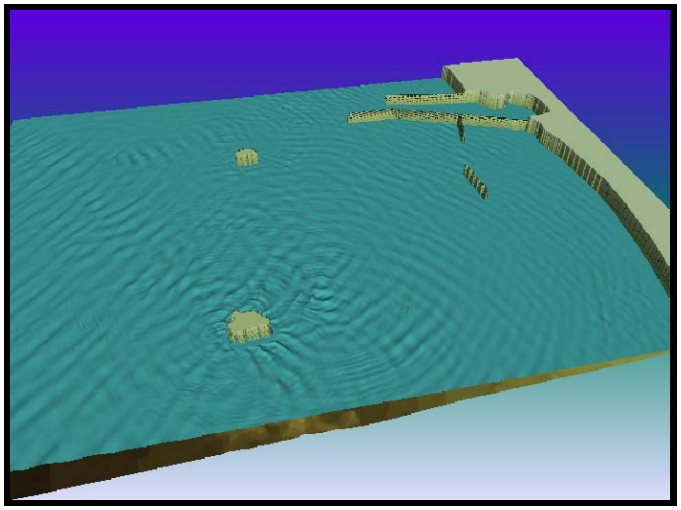

Figure 20. Example sea surface results from the Boussinesq wave model for the combined breakwater and spur jetty alternative.

Figure 21 presents the changes in sediment transport rate, as determined from the radiation flux in the wave modeling results, for three of the final alternatives. The reduction in sediment transport rate was evaluated in three distinct regions along the coast. Areas represented by regions A and B, which are 300-meter (1,000 foot) cells, are currently experiencing significant erosion. Area C, a 600-meter cell, is a region that has exhibited more stable shoreline conditions.

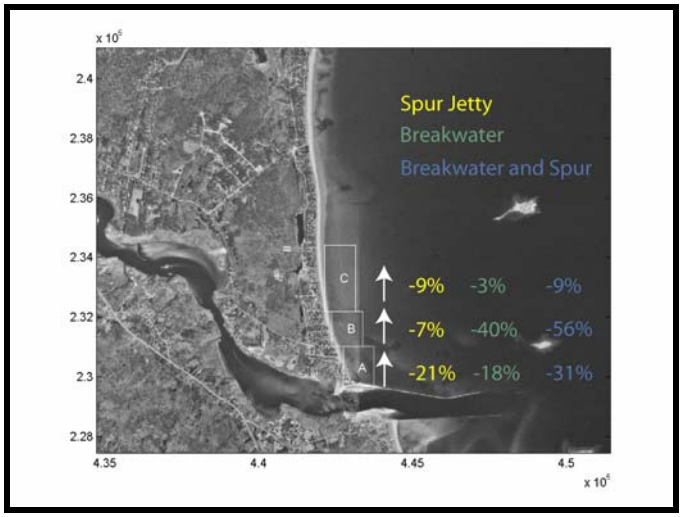

Figure 21. Changes in the sediment transport flux for three of the final alternatives. The numbers indicate the percent reduction in sediment transport rate for each corresponding alternative.

The wave modeling system results were also used to assess the performance of the beach nourishment for existing conditions, and the various final alternatives. Figure 22 presents the performance of a 300,000 cubic yard fill extending 760 meters alongshore for existing conditions (black line), spur jetty alternative (yellow line), breakwater alternative (red line), and combined spur jetty and breakwater alternative (blue line). The vertical axis shows the percentage of material remaining in the region, while the horizontal axis shows the passage of time in years. The upward spike in each alternative on a ten-year interval represents the beneficial re-use of the dredged material (80,000 cubic yards) from the Saco River. The breakwater cases also include the simulated growth of a salient feature behind the structure. The upward trend in the breakwater and combination alternatives indicates the ability to sustain a reasonable beach width and volume through time.

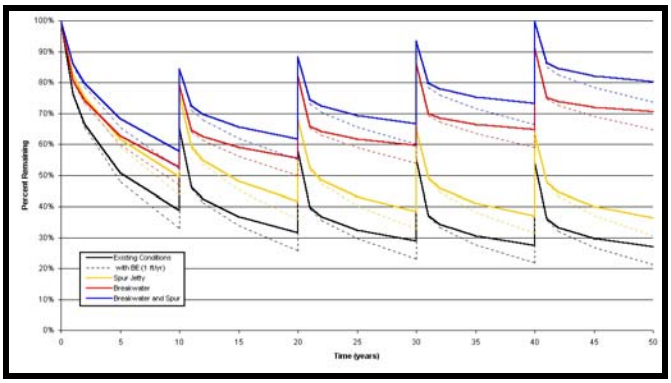

Figure 22. Nourishment performance in erosion areas A and B for existing conditions and various alternatives.

8. CONCLUSIONS

Advanced wave modeling techniques were applied to a practical design setting in Saco, Maine. Wave models were used from generation-scale (utilizing satellite wind data), through transformation-scale, to local scale, to high resolution Boussinesq modeling. Each subsequent model builds on the results from the previous model. The complex nature of the coastal setting required utilization of an in-depth modeling system. Models were calibrated, verified, and/or validated to field measurements at every step of the model progression. Verified models were then utilized to simulate a wide range of shore protection alternatives.

The modeling system involved passing two-dimensional spectra from model to subsequent model, each step resulting in increased resolution, added complexity, and incorporation of additional wave dynamics and structural interactions. Spectral results from the generation-scale model were used as input into STWAVE. Error statistics indicated acceptable errors when compared to field observations. In a similar manner, STWAVE spectral results were used to define boundary conditions for the local wave model (CGWAVE). Error statistics again indicated acceptable errors. The calibration and verification of the models indicated that the spectra was successfully linked and therefore, the model system was able to simulate wave transformations from generation-scale to shoreline impact.

An initial and final screening process was implemented to assess engineering alternatives. The model system was able

to assist in the placement, design, orientation, and evaluation of a wide range of potential solutions. Energy increases and reduction was evaluated as an initial screening mechanism for alternative performance

Wave modeling results were used successfully to generate nearshore currents, sediment transport, and beach nourishment performance for both existing conditions and engineering alternatives.

In all models, utilization of spectra, rather than bulk parameters, are important. For example, increasing the number of spectral components used in CGWAVE results in significant increases in model accuracy.

Additional model enhancements to the Boussinesq model are currently being tested at this location.

Advanced wave modeling and model integration can improve engineering alternatives and design in practical applications. In this particular case, high-level numerical modeling and science functioned not only to understand the physical processes at work, but also produced a design solution to an erosion problem plaguing a community. The use of sound science and advanced modeling also helped unify previously conflicted stakeholders.

ACKNOWLEDGMENTS

The authors thank the U.S. Army Corps of Engineers New England District and Maine Geological Survey for their assistance and support throughout the project planning and progress phases. The authors also thank CR Environmental, Inc. for the bathymetric survey boat, equipment, and operator. The authors also thank Dr. Dave G. Aubrey for his valuable comments. This paper is publication number WHG 2004-011.

REFERENCES

[1] Barber, D.C., Holocene Depositional History and Modern Sand Budget of Inner Saco Bay, ME, Unpublished MS Thesis, University of Maine, Orono, ME, 178 pp., 1995.

[2] Belknap, D.F., Shipp, R.C., Stuckenrath, R., Kelley, J.T., and Borns, H.W., Holocene Sea-Level Change in Coastal Maine, Maine Geol. Surv. Bull, 33: p, 1-21, 1989.

[3] Belknap, D.F., Preservation Potential of the Delaware Atlantic Coast Barrier-Backbarrier System in Kraus, N. C.; Gingerich, K.J.; and Kribel, D.L., eds., Coastal Sediments '91, Proceedings of a Specialty Conference on Quantitative Approaches to Coastal Sediment Processes: New York, Am. Soc. Civ. Eng., v. 2, p. 1269-1283, 1991.

[4] Berkhoff, J.C.W., Mathematical Models for Simple Harmonic Linear Water Waves Wave Refraction and Diffraction, Publ. 163, Delft Hydraulics Laboratory, 1976.

[5] Berkhoff, J.C.W., Computation of Combined Refraction - Diffraction, Proc. 13th International Coastal Engineering Conference, 741-790, 1972.

[6] Bloom, A.L., Late-Pleistocene Fluctuations of Sea Level and Postglacial and Rustal Rebound in Coastal Maine, American Journal of Science, v. 261, p. 862-879, 1963.

[7] Briggs, M.J., Donnell, B.P., Demirbilek, Z., and R.D. Carver, Tediuos Creek Small Craft Harbor: CGWAVE Model Comparisons Between Existing and Authorized Breakwater Configurations., U.S. Army Corps of Engineers ERDC/CHL CHETN-I-67, 2003.

[8] Byrnes, M.R., R.M. Hammer, B.A. Vittor, J.S. Ramsey, D.B. Snyder, J.D. Wood, K.F. Bosma, T.D. Thibaut, N.W. Phillips, Environmental Survey of Potential Sand Resource Sites: Offshore New Jersey. U.S. Department of the Interior, Minerals Management Service, International Activities and Marine Minerals Division (INTERMAR), Herndon, VA. OCS Report MMS 2000-052, Volume I: Main Test 380 pp. + Volume II: Appendices 291 pp., 2000.

[9] Caufield, B.A., and K.F. Bosma, Use of a Large Scale Spectral Wave Generation Model to Define Input into a Nearshore Wave Transformation Model. 8th International Wave Hindcasting and Forecasting Workshop, Oahu, Hawaii, 2004.

[10] Demirbilek, Z. and V.Panchang, CGWAVE: A Coastal Surface Water Wave Model of the Mild Slope Equation. U.S. Army Corps of Engineers technical Report CHL-98-xx, August 1998.

[11] DHI Water and Environment, MIKE 21 Wave Modelling User Guide. DHI Software, 2003.

[12] Dickson, S.M., Kelley, J.T., Belknap, D.F., Fink, L.K., Barber, D.C., FitzGerald, D.M., van Heteren, S., and Manthrop, P.A., A Sediment Budget for Saco Bay, Maine, and an Evaluation of the Long- and Short-Term Geologic and Oceanographic Processes: in List, J.H., ed., Large-scale Coastal Behavior '93: U.S. Geol. Survey Open-File Rept., 93-381, p. 48-51, 1993.

[13] Farrell, Stewart C., Present Coastal Processes, Recorded Changes, and the Post-Pleistocene Geologic Record of Saco Bay, Maine [Unpublished Ph.D. thesis]: University of Massachusetts, 296 p., 1972.

[14] FitzGerald, D.M., I.V. Buynevich, R.A. Davis, Jr., and M.S. Fenster, New England Tidal Inlets with Special Reference to Riverine-Associated Inlet Systems, Geomorphology vol. 48, p., 179-208, 2002.

[15] Forristall, G.Z., Measurements of a saturated range in ocean wave spectra. Journal of Geophysical Research, v. 86, p. 8075-8094, 1981.

[16] Irish, J.L and W.J. Lillycrop, Scanning Laser Mapping of the Coastal Zone, ISPRS Journal of Photogrammetry & Remote Sensing 54, p 123-129, 1999.

[17] Jachec, S.M. and K. F. Bosma, Sediment Transport Related to Potential Sand Mining Offshore New Jersey. Proc. of Waves 2001 Conference, San Francisco, CA. 2001.

[18] Jet Propulsion Laboratory, SeaWinds Science Data Product: User's Manual. Ed. Ted Lungu, California Institute of Technology, 2002.

[19] Jonsson, I.G., Wave-current interactions. *The sea*. Vol. 9, Part A, B. LeMehaute and D.M. Hanes, ed., John Wiley & Sons, Inc., New York, 1990.

[20] Kahma, K.K., A study of the growth of the wave spectrum with fetch. Journal of Physical Oceanography, v. 11, p. 1503-1515, 1981.

[21] Kelley, J.T., Kelley, A.R., Belknap, D.F., and Shipp, R.C., Variability in the Evolution of Two Adjacent Bedrock-Framed Estuaries in Main, In Wolfe, D.A. (editor), Estuarine Variability: Academic Press, Orlando, p. 21-42, 1986.

[22] Kelley, J.T., Shipp, R.C., and Belknap, D.F., Geomorphology and Late Quaternary Evolution of the Saco Bay Region, Maine Geological Survey: Studies in Maine Geology, vol. 5, p. 47-65, 1989.

[23] Kelley, J.T., Belknap, D.F., Fitzgerald, D.M., Barber, D.C., Dickson, S.M., Van Heteren, S., Manthorp, P.A., and Fink, L.K., A Sand Budget for Saco Bay, Maine, Main Geological Survey Open-File Report 95-1, Maine Geological Survey, Augusta, ME, 59 p., 1995.

[24] Kelley, Joseph T. and Anderson Walter A., The Maine Shore and the Army Corps: A Tale of Two Harbors, Wells and Saco, Maine, Maine Policy Review, Fall 2000, pp 20-34, 2000.

[25] Kitaigorodskii, S.A., On the theory of the equilibrium rnage in the spectrum of wind-generated gravity waves. Journal of Physical Oceanography, v. 13, p. 816-827, 1983.

[26] Madsen, P.A. and O.R. Sorenson, A New Form of the Boussinesq Equations with Improved Linear Dispersion Characteristics. Part 2: A Slowly-Varying Bathymetry, Coastal Engineering, 18, pp. 183-204, 1992.

[27] Madsen, P.A., R. Murrary and O.R. Sorensen, A New Form of the Boussinesq Equations with Improved Linear Dispersion Characteristics, Part 1. Coastal Engineering, 15, pp. 371-388, 1991.

[28] Maine State Planning Office, A Study of Beach Processes and Management Alternatives for Saco Bay: Maine State Planning Office Report, Augusta, Maine, 82 p., 1979.

[29] Maine State Planning Office, Improving Maine's Beaches: Recommendations of the Southern Maine Beach Stakeholder Group, Maine State Planning Office Report, Augusta, Maine 1998.

[30] Manthrop, P.A., FitzGerald, D.M., McKinley, P.A., van Heteren, S., and Kelley, J.T., The Effects of Spring Freshets in the Lower Saco River, Maine: Geological Society of America, Abstracts with Programs, v. 26, no. 3, p. 58, 1994.

[31] Manthrop, P.A., Estuarine Circulation and Sediment Transport in the Saco River Estuary, ME, M.S. thesis, Boston University, Boston, MA, 230p., 1995.

[32] Osberg, P.H., Hussey, A.M., II, and Boone, G.M., Bedrock Geologic Map of Maine: Augusta, Maine, Geol. Survey, scale 1:500,000, 1985.

[33] Resio, D.T., The estimation of wind wave generation in a discrete model. Journal of Physical Oceanography, v. 11, p. 510-525, 1981.

[34] Resio, D.T., EXTRM2 Extremes Program User's Guide. Offshore & Coastal Technologies, Inc. (OCTI), 1989.

[35] Resio, D.T., Program WAVAD: Global/Regional Wave Model for Wave Prediction in Deep and/or Shallow Water, Offshore & Coastal Technologies, Inc., 1990.

[36] Saco Bay Regional Beach Management Plan, February 2000.

[37] Smith, J.M, Sherlock, A.R., and D.T.Resio, STWAVE: Steady-State Spectral Wave Model User's Manual for STWAVE, Version 3.0. U.S.Army Corps of Engineers, Vicksburg, MS, 2001

[38] Smith, J.M. and M.B. Gravens, Incident Boundary Conditions for Wave Transformation. 7th International Workshop on Wave Hindcasting and Forecasting, Banff, Alberta, 2002.

[39] Slovinsky, Peter A. and Dickson, Stephen M., Variation of Beach Morphology Along the Saco Bay Littoral Cell An Analysis of Recent Trends and Management Alternatives, Maine Geol. Survey, Open-file Report 03-78, 2003.

[40] Toba, Y., Stochastic form of the growth of wind waves in a single-parameter representation with physical implications. Journal of Physical Oceanography, v. 8, p. 494-507, 1978.

[41] U.S. Army Corps of Engineers, Reports of the Examination and Survey of the Saco River, Executive Document 37, 49th Congress, 1886.

[42] U.S. Army Corps of Engineers, Reports of the examination and Survey of the Saco River, Maine, Document 752, 61st Congress, 1910.

[43] U.S. Army Corps of Engineers, Beach Erosion Control Report in Cooperative Study of Saco, Maine, U.S. Army Corps of Engineers, New England Division, Waltham, MA, 1955.

[44] U.S. Army Corps of Engineers, Camp Ellis Beach, Saco Bay, Maine, Model Study of Beach Erosion, Coastal Model Investigation, U.S. Army engineer division, New England, 1995.

[45] U.S. Army Engineer Waterways Experiment Station, Assessment of Coastal Processes in Saco Bay, Maine, with Emphasis on Camp Ellis Beach, Memorandum, Coastal Engineering Research Center, Vicksburg, MS., 1991.